Three-Dimensional X-Ray Structural Microscopy Using Polychromatic Microbeams

Gene E. Ice and Bennett C. Larson

Abstract

In this article, the authors describe the principle and application of differential-aperture x-ray microscopy (DAXM). This recently developed scanning x-ray microprobe technique uses a confocal or traveling pinhole camera approach to determine the crystal structure, crystallographic orientation, and elastic and plastic strain tensors within bulk materials. The penetrating properties of x-rays make the technique applicable to optically opaque as well as transparent materials, and it is nondestructive; this provides for *in situ*, submicrometer-resolution characterization of local crystal structure and for measurements of microstructure evolution on mesoscopic length scales from tenths to hundreds of micrometers. Examples are presented that illustrate the use of DAXM to study grain and subgrain morphology, grain-boundary types and networks, and local intra- and intergranular elastic and plastic deformation. Information of this type now provides a direct link between the actual structure and evolution in materials and increasingly powerful computer simulations and multiscale modeling of materials microstructure and evolution.

Keywords: *deformation, microdiffraction, polychromatic microbeams, three-dimensional differential-aperture x-ray microscopy (DAXM).*

Introduction

Most solid materials are crystalline, with grain sizes ranging from nanometers to hundreds of micrometers. The misoriented grains of polycrystals are connected by networks of grain boundaries with distinct local crystallography and anisotropic physical properties. Understanding the behavior of polycrystalline materials under thermal, mechanical, chemical, and electrical stresses and predicting the consequences of advanced technological processing techniques represent a longstanding materials research goal.[1–3] Despite remarkable progress, predicting new materials, microstructure, and evolution is not yet possible. Finite element modeling (FEM) using constitutive relations and continuum mechanics has revolutionized the design and manufacture of structural components over length scales where mesoscopic structure can be ignored.[4] The development of analogous theory and modeling capabilities for mesoscopic length scales has proven to be extremely difficult because of the complex and collective inter- and intragranular microstructural interactions.[4–6]

Transmission electron microscopy (TEM) provides detailed microstructural information on thin-section samples,[6,7] and electron backscattering diffraction (EBSD) is readily available[8,9] for micrometer- and submicrometer-resolution surface structure, microstructure, and deformation measurements. However, these thin-section and surface tools are not designed for detailed testing of computer simulations and multiscale modeling of the evolution of materials microstructure in three dimensions. Direct, nondestructive measurements are needed of the local microstructure and evolution in the interior of bulk materials on mesoscopic length scales of tenths of microns to hundreds of microns.

The ongoing development of advanced high-resolution x-ray imaging and diffraction techniques is beginning to fill this need. As illustrated in the article by Schroer et al. in this issue of *MRS Bulletin,* absorption and fluorescence microtomography techniques are providing nondestructive mass and chemical-specie-sensitive spatial distributions with submicrometer resolution in three dimensions on a wide range of materials. Robust and rapid high-energy diffraction techniques have been developed that can provide ~5-μm-resolution measurements of crystal grains, grain orientations, and microstructural features over length scales of millimeters or more.[10,11] Moreover, techniques for the direct inversion of coherent diffraction patterns from samples with sizes on the order of a micrometer and smaller are now pushing three-dimensional (3D) x-ray spatial resolution of objects down to a few nanometers.[12,13]

In this article, we focus on the development and application of differential-aperture x-ray microscopy (DAXM), a polychromatic x-ray microbeam diffraction technique for studying local crystal structure, orientation, and strain tensors without crystal rotation.[14] This technique provides submicrometer point-to-point spatial resolution in three dimensions over length scales from tenths to hundreds of micrometers. The "structural" aspect of DAXM refers not only to the local crystallographic structure probed within submicrometer volumes, but also to the construction of 3D maps of local crystal microstructure on mesoscopic length scales. DAXM is particularly well suited for micrometer- and submicrometer-resolution microstructure investigations involving intra- and intergranular microstructure and evolution on mesoscopic length scales.

Polychromatic X-Ray Structural Microscopy

Polychromatic structural microscopy[15] is a spatially resolved diffraction technique based on Laue diffraction, the oldest x-ray diffraction method. As illustrated schematically in Figure 1, x-ray beams with an energy range of 8–20 keV generate diffraction patterns with 10–20 reflections from simple fcc or bcc single crystals; more reflections are generated if the unit cell is larger.[16] These reflections are associated

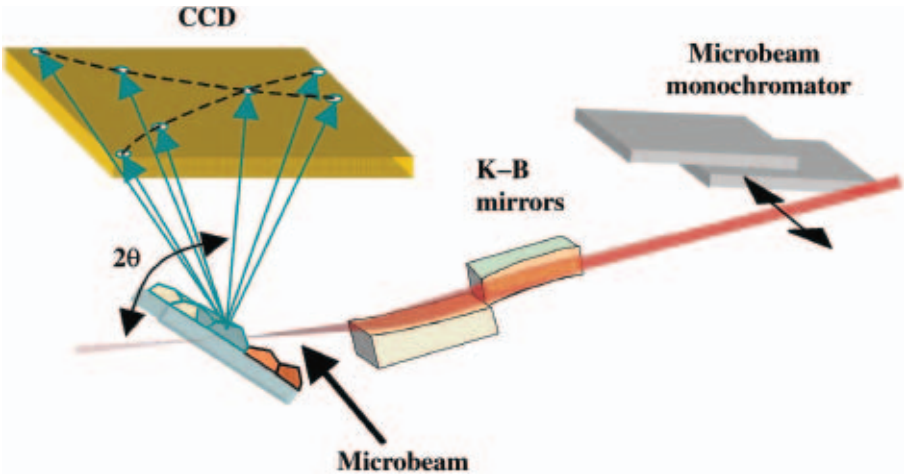

Figure 1. Schematic illustration of a polychromatic x-ray structural microscope in which polychromatic x-rays are focused to a submicrometer spot diameter onto the sample position using crossed Kirkpatrick–Baez (K–B) mirrors. The Laue diffraction patterns are detected using a CCD x-ray area detector. An insertable/removable double-crystal monochromator is shown that provides for wavelength-tuneable monochromatic microbeams if desired.

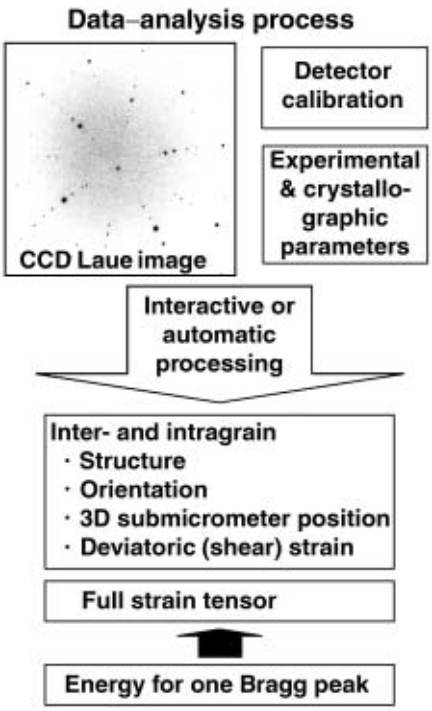

Figure 2. Flow diagram of the data-analysis procedure in which 2D or 3D spatially resolved Laue diffraction patterns are indexed and analyzed to obtain microstructural information.

with sets of internal crystal planes that act as x-ray mirrors with negligible reflectivity, except for wavelengths and incident angles that simultaneously satisfy the constructive interference (Bragg) condition:

$$\lambda = 2d \sin(\theta). \quad (1)$$

Here, d is the distance between crystal planes, θ is the mirror reflection angle, and 2θ is the total scattering angle.

In Figure 1, a polychromatic (or optional monochromatic) synchrotron x-ray beam is focused, using nondispersive total external reflection Kirkpatrick–Baez mirrors, to a submicrometer-diameter spot onto the thin-film sample.[17] Differential deposition,[18,19] differential bending,[20] or differential polishing methods can all be used to produce high-precision elliptical mirrors to focus beams to spot sizes of ~0.1–0.5 μm; a depth of field of up to ~0.5 mm is possible. Different regions of the sample are probed by translating the sample under the beam.

The Laue patterns from subgrains that intercept the beam are detected by an x-ray-sensitive CCD area detector placed normal to the incident beam. For cubic crystals, the Bragg plane spacing d is given in terms of the lattice parameter a_0 and the (hkl) indices by

$$d = a_0/(h^2 + k^2 + l^2)^{1/2}; \quad (2)$$

the angles between Bragg spots are given by the scalar product of the plane normals.

The central data-analysis problem of polychromatic x-ray structural microscopy is the determination of the indices (hkl) of the Laue reflections. As outlined in Figure 2, this "indexing" is carried out by computer, searching the Bragg peaks in the diffraction images for patterns of angles that match those expected for the sample.[16]

Precision analysis of the angles between reflections is used to determine deviatoric (shear) strain tensor components (ε_{ij}) with an uncertainty of $\sim 1 \times 10^{-4}$. The deviatoric strain tensor reflects distortions in the shape of unit cells as a result of changes in the angles between crystallographic planes and in the relative lengths of cell vectors resulting from shear stresses. In order to measure the volume change of the unit cell (dilatational strain), a nondispersive monochromator[21] is inserted in front of the focusing mirrors, and the energy is scanned to find the energy of one of the reflections (see Figure 1).

Three-Dimensional X-Ray Structural Microscopy

Submicrometer-diameter beams automatically provide submicrometer spatial resolution in the two dimensions normal to the beam. Figure 3 illustrates the method of obtaining submicrometer spatial resolution *along* the direction of the beam; until recently, this was an unsolved problem in x-ray diffraction.[14,22] In general, simple slit techniques do not work for micrometer resolution because hard x-rays require slit blades of >10 μm thickness; a 1-μm-wide slit with 10-μm-thick blades would act as a collimator and could not pass the large angular crossfire of the diffraction patterns. However, the use of an absorbing wire (with its circular cross section) as a differential-aperture (i.e., knife-edge) slit makes it possible to obtain micrometer or submicrometer resolution and still pass the highly divergent x-ray patterns to the CCD area detector.[14] As illustrated by Figure 3, the circular cross section of the wire presents the same absorption profile for x-rays of all angles; therefore, by taking the circular profile as well as the center position of the wire into account in the computer analysis, it is possible to get the effect of a micrometer-resolution hard x-ray aperture.

By locating the Pt wire profiler close to the sample and using the difference between the CCD diffraction pattern images taken before and after small (micrometer or submicrometer) steps of the wire, the diffracted beam intensity passing through the step-advance distance can be obtained. The origin of this intensity for both intra- and intergranular Bragg reflected beams is determined by geometric triangulation from the position of a (typically ~20 × 20 μm^2) CCD pixel to the position of the leading edge of the Pt wire and extrapolating from the wire down to the intersection with the microbeam. After stepping the profiler through the entire diffraction pattern, computer collation makes it possible to reconstruct a complete

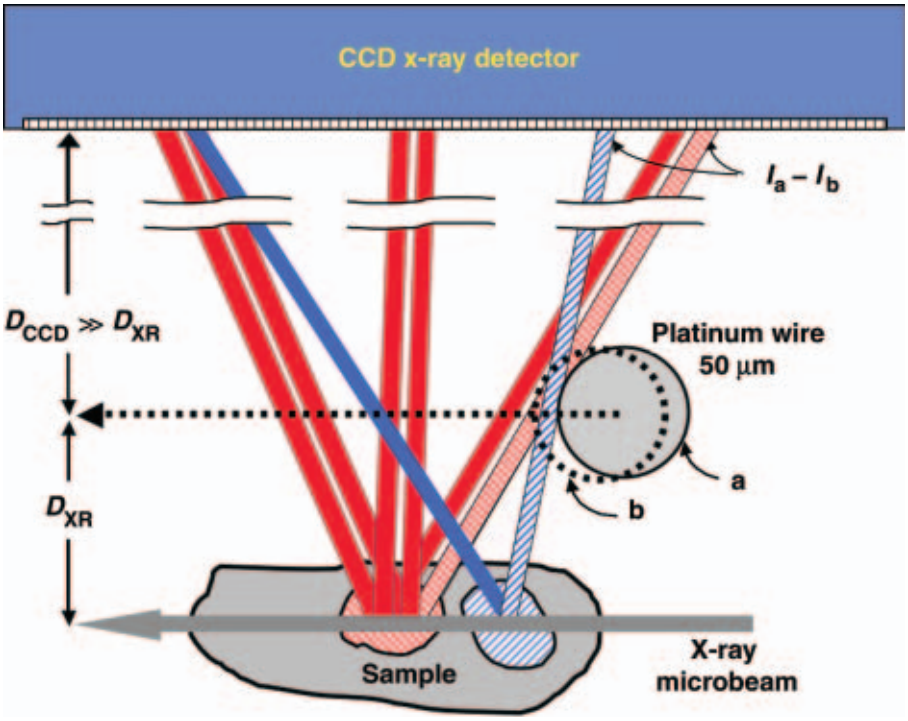

Figure 3. Schematic illustration of the differential-aperture x-ray microscopy (DAXM) technique to obtain inter- and intragranular Laue diffraction patterns from submicrometer increments along the microbeam. D_{CCD} is the distance from the detector to the profiler wire, and D_{XR} is the distance from the x-ray microbeam to the profiler wire. The intensity change between images collected with the wire at positions a and b provides the intensity $I_a - I_b$ (hatched areas). The intercept of the CCD pixel/wire-edge ray and the incident beam determines the origin of the intensity difference.

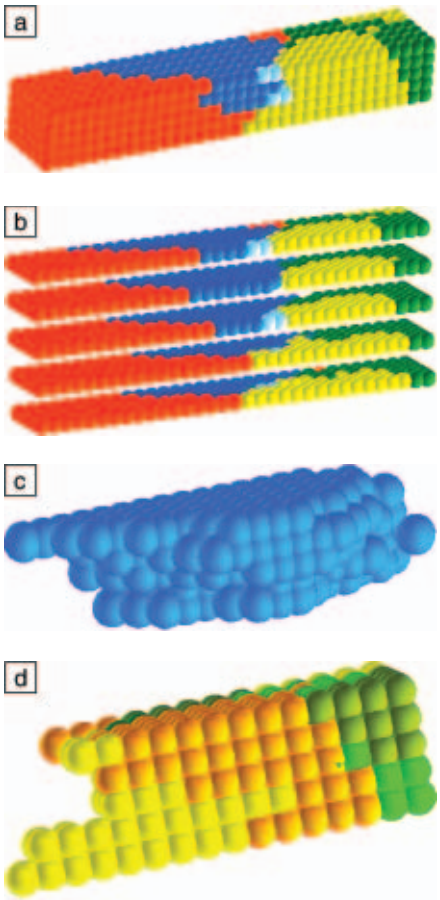

Figure 4. Three-dimensional orientation mapping of crystal grains in an Al polycrystal obtained using DAXM. The color-coded marker positions correspond to micrometer spacing in each direction. (a) Array (6 × 5 × 33) of micrometer-spaced measuring points, showing two larger grains (red and blue) and several smaller grains; (b) same array as in (a), but with the vertical axis expanded to show inner structure; (c) enlargement of the blue grain in (a), showing morphology and absence of subgrains; and (d) enlargement of green and yellow grains in (a), where the different shadings show the presence of subgrains.

(single-crystal) CCD diffraction pattern for each depth position along the microbeam.

Since each scan of the profiling wire provides information along a single line, 3D structural images of materials are compiled by translating the sample over a lateral array of positions with micrometer or submicrometer step sizes. Wire profiler scans typically entail 300–400 steps, with 2–3 s per wire step, limited by the detector readout time. The computer reconstruction and analysis of the diffraction patterns for each increment along the beam requires ~30 min on a desktop computer. Decreasing these times by a factor of 10 or more is possible with the use of faster detectors and computer clusters.

Obtaining full Laue diffraction patterns for submicrometer-resolution voxels (3D volume elements) means that full diffraction information is available with point-to-point submicrometer spatial resolution. This result is fundamentally important; it means that DAXM can be applied to single-crystal, polycrystalline, composite, and functionally graded materials, and to both elastically and plastically deformed materials. Moreover, as discussed earlier, the single-crystal Laue diffraction patterns obtained at each position provide not only the crystal phase and orientation of the diffracting material, but also the elastic strain tensors. It is important for the DAXM technique using submicrometer-diameter microbeams that full diffraction patterns are obtained from each segment along the beam without sample rotation. Only the point at the center of rotation would remain within the submicrometer width of the x-ray beam if the sample were rotated (see Figure 3).

Applications of DAXM to Three-Dimensional X-Ray Microstructures

Polycrystalline Grain Structure

Figure 4 provides an initial example of 3D submicrometer-resolution DAXM imaging of local grain structure, where an Al(1at.%Fe,Si) polycrystal was probed using DAXM, and the grain orientations determined were coded by color for display.[23] Local crystal orientation measurements were obtained over the 3D volume shown by performing DAXM line scans on a 5 × 6 array of points with 1 μm lateral spacing. The 3D array of diffraction patterns for the 5 μm × 6 μm × 33 μm volume of the sample shown was computer-indexed and analyzed to obtain the local crystal orientation for each point. Figure 4a is an opaque, color-coded representation of local crystal orientations for each of the 990 sites in the volume; this provides a micrometer-resolution 3D computer map of the grain orientations, sizes, and morphologies. In Figure 4b, the layers have been separated vertically to reveal the interior of the grains within the measured volume. Since the orientations at each point are determined to an angular accu-

racy of ~0.01°, detailed information on the presence of subboundaries and rotational (i.e., plastic) strain within grains is available as well. Figure 4c shows the morphology of the blue grain isolated from the full volume; the variation of angular orientation is less than 0.1° within this grain. Figure 4d shows the presence of subgrains within the yellow and green grains by enhancing the angular sensitivity of the false-color images; the subgrains displayed have angular variations of ~0.5°. These results demonstrate the potential for investigating a wide range of size and morphology characteristics of grains, grain boundaries, grain-boundary junctions, and intra- as well as intergranular subgrain and plastic deformation distributions. Fundamental investigations of thermal grain growth in three dimensions are in progress using this technique.

Strain Tensors and Strain Gradients

Figure 5 demonstrates the ability of DAXM to depth-resolve diffraction patterns that have continuously varying rotations. The length of the elongated diffraction spots in the "depth-integrated" Laue diffraction pattern (Figure 5a, top) indicates the angular range of rotations encountered by the beam as it penetrated through the silicon plate cylindrically bent to a radius R of 3.3 mm; however, the streaks do not provide information on the depth distribution of the rotations. Figure 5a (bottom) shows superimposed "depth-resolved" diffraction patterns obtained using DAXM for two positions along the beam penetration direction. The depth positions correspond to a 1 μm increment at the top surface and a 1 μm increment at the bottom surface of the 25-μm-thick sample. As emphasized by the enlarged views of the (008) and ($\bar{3}$,1,11) Laue reflections in Figure 5a (bottom), two separate spots now appear at positions corresponding to the end points of the elongated streaks in the depth-integrated diffraction pattern in (Figure 5a, top). Therefore, DAXM provides full diffraction patterns for micrometer depth increments that can be analyzed to obtain both the orientation and the elastic strain state for each depth increment.

Since Si is brittle and does not plastically deform at room temperature, a large elastic tensile strain is generated in the x direction at the top surface, and a large compressive strain is generated in the x direction at the bottom surface (see Figure 5b). Figure 5c shows the depth-dependence of the deviatoric strain for the bent Si (symbols) and for a flat Si single crystal (lines). The strain along the bend direction is large and positive at the top (~3 × 10^{-3}) and large and negative at the bottom. The solid lines are the results of similar strain measurements made on a flat (i.e., unstrained) sample; the fluctuations around zero show the ~10^{-4} uncertainties in the strain measurements. Since the y component of the full (dilatational plus deviatoric) strain vanishes for cylindrical bends, the ε'_{yy} values provide a direct measurement of the homogeneous dilatation strain as a function of depth. The fact that ε'_{yy} is not zero indicates the presence of shear stresses generated by the cylindrical bend.

Obtaining full diffraction patterns for submicrometer voxels in three dimensions is key to the DAXM technique; this result demonstrates that local orientations and strains can be determined simultaneously, even under the most general conditions, including continuous gradients.

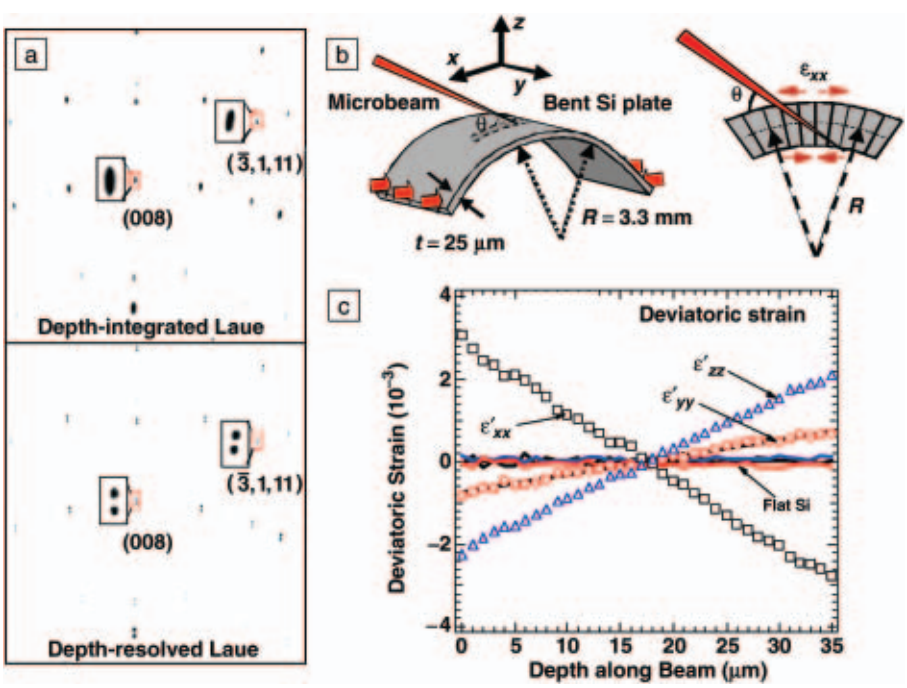

Figure 5. (a) Depth-integrated and depth-resolved Laue diffraction patterns. (b) Schematic illustrations of the geometry for spatially resolved measurement of the orientation and strain tensors in a cylindrically bent Si plate; t *is the thickness of the bent plate,* R *is the radius of the bent plate, and* ε_{xx} *is the normal strain in the* x *direction. (c) Depth-resolved measurements of the diagonal components of the deviatoric strain tensor, providing the normal deviatoric strain in the* x, y, *and* z *directions. The solid lines show data for the flat Si plate, while the symbols are data for the bent Si sample.*

Monochromatic DAXM

An energy-scanning monochromatic adaptation[24] of DAXM has been developed that is complementary to the polychromatic technique in that it provides absolute lattice parameters. By inserting the monochromator into the synchrotron x-ray beam before it strikes the K–B mirrors (see Figure 1), a monochromatic microbeam is focused onto the sample. This makes it possible to perform an energy versus depth scan on a single Bragg reflected beam; knowledge of the beam energy (wavelength λ) and measurement of the scattering angle 2θ determine the lattice spacing using the Bragg equation described earlier. This mode is fully 3D and provides the absolute lattice parameter and tilt orientation of the Bragg reflecting plane as a function of depth along the microbeam. Monochromatic DAXM measurements have been demonstrated in a study of the surface normal (ε_{zz}) strain and anticlastic bending in cylindrically bent Si plates.[24] Monochromatic DAXM will likely find wide application, as it does not require a white (i.e., polychromatic) beam and is generally simpler to perform than the polychromatic DAXM technique.

Plastic Deformation Microstructure under Nanoindents

The ability to extract local lattice orientations from a continuous distribution of orientations provides a direct nondestructive technique for investigating plastic deformation in ductile materials.[25–28] Figure 6 provides an overview of how polychromatic DAXM measurements yield direct, quantitative information on lattice rotations along the microbeam direction. Fig-

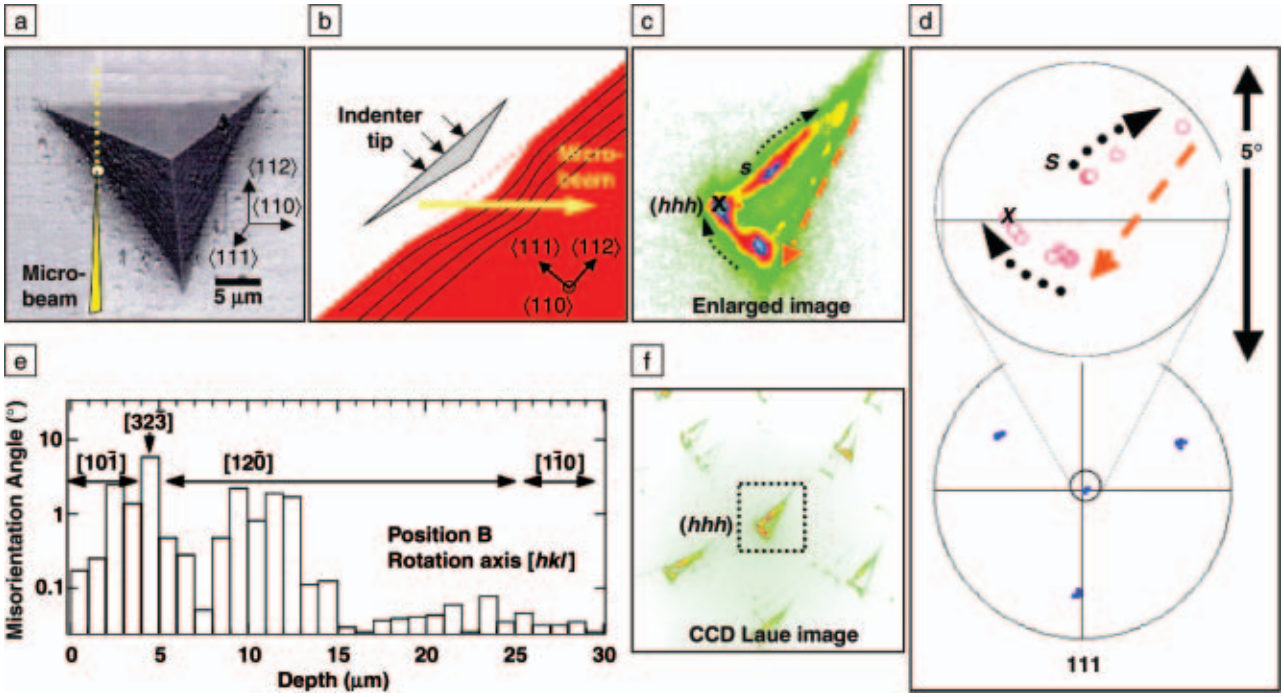

*Figure 6. (a) Atomic force micrograph of a Berkovich (pyramid-shaped) nanoindent in a Cu single crystal. (b) Schematic illustration of the probe geometry of the microbeam. (c) Laue diffraction pattern of the indent. (d) DAXM analysis of the streaked diffraction pattern in (c), plotted quantitatively in degrees; (e) log-scale plot of rotations per micrometer and rotation axes; and (f) enlarged (*hhh*) reflection for the microbeam position. See text for details.*

ure 6a depicts a microbeam entering the surface of a Berkovich (pyramid-shaped) nanoindent in a Cu single crystal.[27,28] Figure 6b shows a side-view schematic of the microbeam as local Bragg reflections probe the lattice rotations as a function of depth under the sharp edge of the indenter. Since polychromatic beams produce a specular (mirrorlike) Bragg reflection off lattice plane orientations at each depth, the triangular shape of the Laue diffraction spots in Figures 6c and 6f signifies a complex and highly inhomogeneous "distribution" of local lattice rotations as a function of depth under the indenter. This complex pattern (with strong intensity variations incorporated in the triangular streaks) is in strong contrast to the simple streak pattern associated with the small, continuous, one-dimensional rotations as a function of depth observed for the cylindrically bent Si in Figure 5. However, just as was demonstrated for the top and bottom micrometer-depth layers of Si in Figure 5, each micrometer of depth in the indented Cu produces a complete Laue diffraction pattern with a particular orientation that is extracted by the DAXM profiling analysis.[28] For instance, the DAXM analysis of the streaked diffraction pattern (plotted quantitatively in degrees in Figure 6d) showed that the lattice orientation at the surface (i.e., where the microbeam entered the sample) corresponds to a rotation of the Bragg reflection to position *s* (surface) in Figures 6c and 6d. The DAXM analysis in Figure 6d indicates that the indent deformation rotates the lattice several additional degrees in the next 3 μm (upward along the dotted arrow from point *s*) indicated by the four micrometer-spaced open-circle symbols. Since no circles appear along the direction of the downward-pointing dashed arrow in Figures 6c and 6d, it can be inferred that the lattice rotates 6.5° in less than 1 μm at this depth. The fact that the orientations (i.e., circles in Figure 6d) return to near the undeformed position (*x*) for depths of about 12–15 μm into the crystal indicates that the indent deformation is quite small at these depths and this position. The micrometer-by-micrometer lattice orientation changes are presented quantitatively in Figure 6e, where the magnitude of the angular misorientations along the beam direction are plotted on a log scale. The approximate crystallographic axis of rotation is indicated for each step as well, showing several well-defined rotation axes with sharp changes in direction.

The important point is that DAXM profiling provides complete orientation information for each micrometer step along the beam. By making such measurements on an array surrounding the indented area, the entire deformation pattern below the indenter can be determined quantitatively with micrometer resolution in three dimensions. This type of data provides direct information for fundamental studies of the deformation process and a direct input for comparison with finite element and multiscale modeling of deformation under indents and testing of strain-gradient theories.[3–5,29,30]

Thin-Film Layered Structures

Epitaxial thin films on crystalline substrates, buffer layers between films and substrates, and barrier-coated substrates represent large classes of technologically important film structures.[31,32] Penetrating x-ray microbeams make it possible to obtain, simultaneously, epitaxy and grain-structure information on thin films, buffer layers, and substrates from their superimposed Laue patterns without direct depth resolution. For instance, grain-by-grain microbeam diffraction studies of the epitaxy of CeO_2 films on roll-textured Ni substrates have provided combinatorial-like information on the surface–miscut angle-dependent (i.e., vicinal angle) epitaxy of CeO_2 on Ni grains.[33] The changes in intergranular rotation induced by the spe-

cific CeO_2 epitaxy have been used to calculate the improvement in percolation (continuity) paths for superconducting currents, using 5° as the limit for weak-link generation.

Figure 7 shows[33] that the changes can be significant as 2D percolation paths (paths of continuity denoted by continuous regions of a single color in both vertical and horizontal directions) arise within the intergranular orientations of CeO_2 buffer layers on Ni, while percolation paths based on the intergranular orientations of the vicinal Ni surfaces provide only 1D (horizontal, in this case) percolation paths. Although a number of important 2D or pseudo-3D x-ray microbeam investigations have been performed,[34,35] they are outside the focus of 3D microscopy in this article.

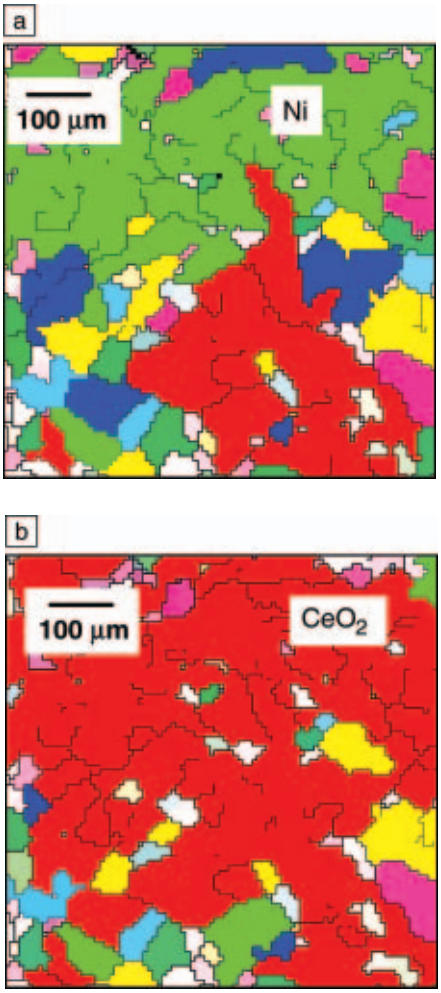

Figure 7. (a), (b) Orientation maps for Ni substrate and epitaxial CeO_2 film produced by x-ray microdiffraction; the lines represent grain boundaries. Areas of a particular color denote regions in which all grain boundaries have rotations of less than 5° and therefore do not disrupt current flow. Grain boundaries associated with color changes have rotations of more than 5° and disrupt current flow; thus, continuous current flow paths exist both vertically and horizontally in (b), while only a horizontal path would have been available if the Ni substrate orientations in (a) were retained.

Future Outlook

X-ray structural microscopy is still in its infancy as compared with, for example, transmission electron microscopy, which has been under development for some 50 years and is still experiencing remarkable advances. Similarly, electron backscattering microscopy is now a relatively mature technique that remains the subject of ongoing and rapid advancements. As the development of synchrotron sources, x-ray focusing optics, CCD detectors, and advanced x-ray structural diffraction and analysis methods continue, x-ray structural microscopy techniques can be expected to become both more powerful and easier to apply and, as a result, to find wide application.

For optimizing the DAXM technique, the development of parallel depth-profiling schemes will be important, as will advanced data handling and analysis techniques to obtain near-real-time visualization of results. Of even greater importance, however, will be the design of new types of experiments in concert with theory, computer simulations, and multiscale modeling, so that observations of material microstructure and evolution can be used to provide critical tests of fundamental materials issues on mesoscopic length scales.[4,5,29,30]

Acknowledgments

We gratefully acknowledge the contributions of Wenge Yang, N. Tamura, J.-S. Chung, W. Liu, J.D. Budai, J.Z. Tischler, P. Zschack, W. Lowe, and E. Dufresne. This work was performed on the UNICAT and MHATT-CAT beamlines at the Advanced Photon Source (APS). Research was supported by the U.S. DOE Office of Science, Basic Energy Sciences, Division of Materials Sciences, under contract with Oak Ridge National Laboratory, managed by UT-Battelle, LLC. The UNICAT facility at the APS is supported by the DOE under award DEFG02-91ER45439, through the Frederick Seitz Materials Research Laboratory at the University of Illinois at Urbana-Champaign, the Oak Ridge National Laboratory (DOE contract DE-AC05-00OR22725 with UT-Battelle LLC), the National Institute of Standards and Technology (U.S. Department of Commerce) and UOP LLC. Operation of the MHATT-CAT Sector 7 beamlines at the APS was supported by DOE grant DE-FG02-99ER45743. The APS is supported by the DOE, Basic Energy Sciences, Office of Science, under contract W-31-109-ENG-38.

References

1. M. Demirel, A.P. Kuprat, D.C. George, and A.D. Rollett, *Phys. Rev. Lett.* **90** 016106 (2003).
2. B. Devincre, L.P. Kubin, C. Lemarchand, and R. Madec, *Mater. Sci. Eng., A* **A309** (2001) p. 211.
3. P.R. Dawson, *Int. J. Sol. Struct.* **37** (2000) p. 115.
4. A. Needleman, *Acta Mater.* **48** (2000) p. 105.
5. A. El-Azab, *Phys. Rev. B* **61** 11956 (2000).
6. N. Hansen, *Metall. Mater. Trans. A* **32A** (2001) p. 2917.
7. D.A. Hughes and N. Hansen, *Acta Mater*. **45** (1997) p. 3871.
8. F.J. Humphreys, *J. Mater. Sci.* **36** (2001) p. 3833.
9. A.J. Schwartz, M. Kumar, and B.L. Adams, *Diffraction in Materials Science* (Kluwer Academic/Plenum, New York, 2000).
10. H.F. Poulsen, L. Margulies, S. Schmidt, and G. Winther, *Acta Mat.* **51** (2003) p. 3821.
11. L. Margulies, G. Winther, and H.F. Poulsen, *Science* **291** (2001) p. 2392.
12. J. Miao, T. Ishikawa, B. Johnson, E.H. Anderson, B. Lai, and K.O. Hodgson, *Phys. Rev. Lett.* **89** 088303 (2002).
13. G.J. Williams, M.A. Pfeifer, I.A. Vartanyants, and I.K. Robinson, *Phys. Rev. Lett.* **90** 175501 (2003).
14. B.C. Larson, W. Yang, G.E. Ice, J.D. Budai, and J.Z. Tischler, *Nature* **415** (2002) p. 887.
15. G.E. Ice and B.C. Larson, *Adv. Eng. Mater*. **2** (2000) p. 643.
16. J.-S. Chung and G.E. Ice, *J. Appl. Phys*. **86** (1999) p. 5249.
17. G.E. Ice, J.-S. Chung, J.Z. Tischler, A. Lunt, and L. Assoufid, *Rev. Sci. Instrum.* **71** (2000) p. 2635.
18. C. Liu, R. Conley, L. Assoufid, A.T. Macrander, G.E. Ice, J.Z. Tischler, and K. Zhang, *J. Vac. Sci. Technol., A* **21** (2003) p. 1579.
19. K. Yamauchi, K. Yamamura, H. Mimura, Y. Sano, A. Saito, A. Souvorov, M. Yabashi, K. Tamasaku, T. Ishikawa, and Y. Mori, *J. Synch. Rad.* **9** (2002) p. 313.
20. O. Hignette, P. Cloetens, W.K. Lee, W. Ludwig, and G. Rostaing, *J. Phys. IV* (France) **104** (2003) p. 231; O. Hignette (private communication).
21. G.E. Ice, J.-S. Chung, W. Lowe, E. Williams, and J. Edelman, *Rev. Sci. Instrum*. **71** (2000) p. 2001.
22. G.S. Cargill, *Nature* **415** (2002) p. 844.
23. W. Yang, B.C. Larson, J.Z. Tischler, G.E. Ice, J.D. Budai, and W. Liu, *Micron* (2004) in press.
24. W. Yang, B.C. Larson, G.E. Ice, J.Z. Tischler, J.D. Budai, K.-S. Chung, and W.P. Lowe, *Appl. Phys. Lett.* **82** (2003) p. 3856.
25. R.I. Barabash, G.E. Ice, B.C. Larson, G.M. Pharr, K.-S. Chung, and W. Yang, *Appl. Phys. Lett.* **79** (2001) p. 749.
26. B.C. Larson, W. Yang, J.Z. Tischler, J.D. Budai, W. Liu, and H. Weiland, *Int. J. Plasticity* **20** (2004) p. 543.
27. W. Yang, B.C. Larson, G.M. Pharr, G.E. Ice, J.D. Budai, J.Z. Tischler, and W. Liu, *J. Mater. Res.* **19** (2004) p. 66.

28. W. Yang, B.C. Larson, G.M. Pharr, G.E. Ice, J.Z. Tischler, J.D. Budai, and W. Liu, in *Multiscale Phenomena in Materials—Experiments and Modeling Related to Mechanical Behavior*, edited by K.J. Hemker, D.H. Lassila, L.E. Levine, and H.M. Zbib (Mater. Res. Soc. Symp. Proc. **779,** Warrendale, PA, 2003) p. W5.34.1.
29. H. Gao, Y. Huang, and W.D. Nix, *Naturwissenschaften* **86** (1999) p. 507.
30. M.C. Fivel, C.F. Robertson, G.R. Canova, and L. Boulanger, *Acta Mater.* **46** (1998) p. 618.
31. D.P. Norton, A. Goyal, J.D. Budai, D.K. Christen, D. Kroeger, E. Specht, Q. He, B. Saffian, M. Paranthaman, C. Klabunde, D. Lee, B.C. Sales, and F. List, *Science* **274** (1996) p. 755.
32. A. Goyal, D.P. Norton, J.D. Budai, M. Paranthaman, E.D. Specht, D.M. Kroeger, D.K. Christen, Q. He, B. Saffian, F.A. List, D.F. Lee, P.M. Martin, C.E. Klabunde, E. Hartfield, and V.K. Sikka, *Appl. Phys. Lett.* **69** (1996) p. 1795.
33. J.D. Budai, W. Yang, N. Tamura, J.-S. Chung, J.Z. Tischler, B.C. Larson, G.E. Ice, C. Park, and D.P. Norton, *Nat. Mater.* **2** (2003) p. 487.
34. R. Spolenak, W.L. Brown, N. Tamura, A.A. MacDowell, R.S. Celestre, H.A. Padmore, B. Valek, J.C. Bravman, T. Marieb, H. Fujimoto, B.W. Batterman, and J.R. Patel, *Phys. Rev. Lett.* **90** 0961021 (2003).
35. N. Tamura, A.A. MacDowell, R.S. Celestre, H.A. Padmore, B. Valek, J.C. Bravman, R. Spolenak, W.L. Brown, T. Marieb, H. Fujimoto, B.W. Batterman, and J.R. Patel, *Appl. Phys. Lett.* **80** (2002) p. 3724. □

Advertisers in This Issue

	Page No.
Advanced Metallization Conference (AMC) 2004	211
* Aldrich Chemical Company, Inc.	146
* American Scientific Publishers	139
* Andeen-Hagerling, Inc.	138
Annual Reviews	203
* Asylum Research	151
* Bruker AXS, Inc.	129
* Chemat Technology, Inc.	137
* EDAX, Inc.	148
* Gatan, Inc.	133
**Genentech, Inc.	142
Goodfellow Corp.	165
High Voltage Engineering	Inside front cover
* Huntington Mechanical Labs, Inc.	Outside back cover
* Hysitron, Inc.	141
* JEOL USA, Inc.	134
* LEO Electron Microscopy, Inc.	147
* MMR Technologies, Inc.	201
* Molecular Metrology, Inc.	176
* MTS Systems Corp.	Inside back cover
* NanoInk, Inc.	130
* National Electrostatic Corp.	140
Pacific Nanotechnology, Inc.	138
* PANalytical, Inc.	181
Smart Imaging Technologies	143
**Sun Microsystems, Inc.	145

For free information about the products and services offered in this issue, check
http://advertisers.mrs.org

Please visit us at the Exhibit or Career Center**, April 13–15, during the 2004 MRS Spring Meeting in San Francisco.*

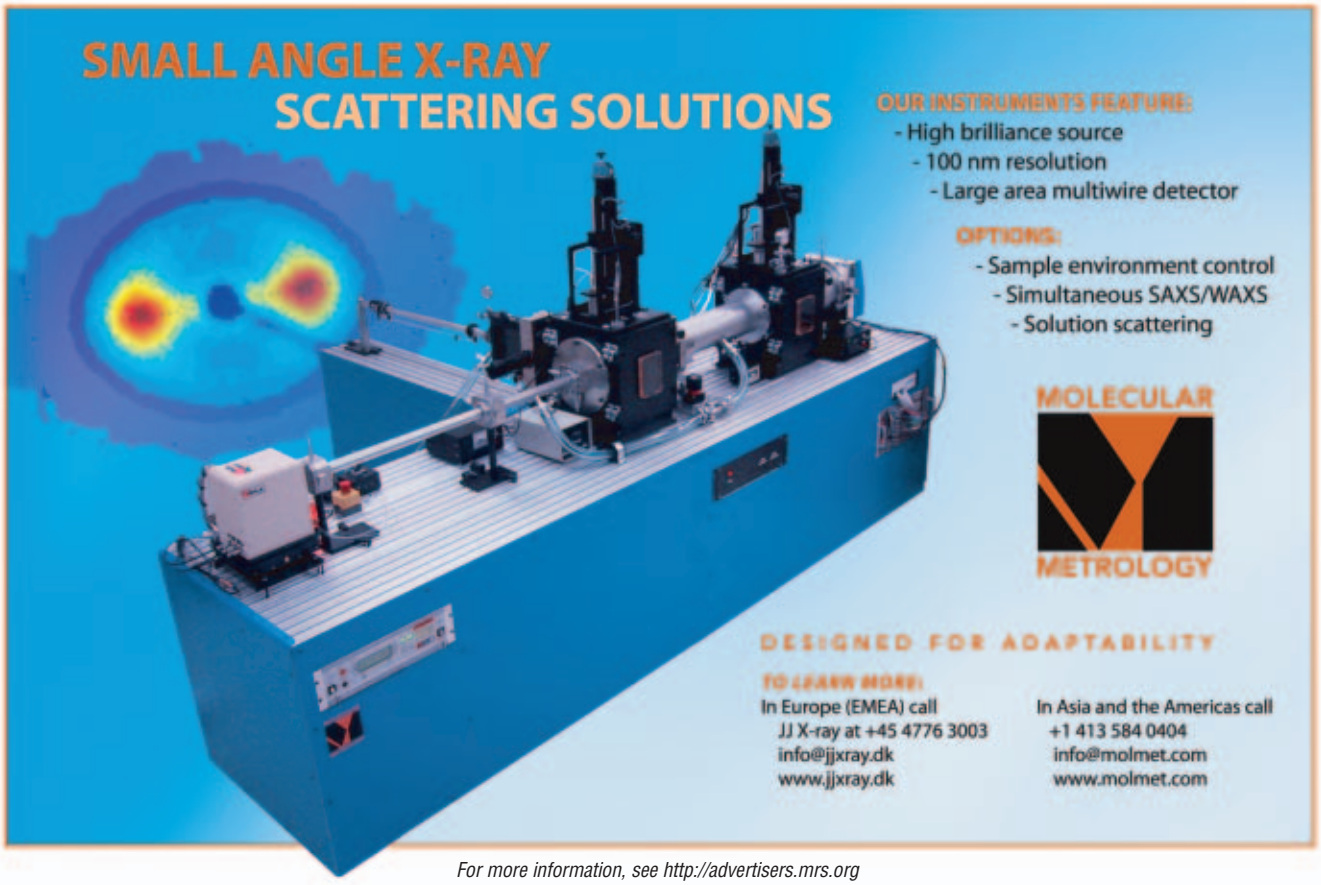

For more information, see http://advertisers.mrs.org